*Korean J. Chem. Eng.*, **28**(5), 1221-1226 (2011)
DOI: 10.1007/s11814-010-0486-y

# Nanoclays as nano adsorbent for oxidation of $H_2S$ into elemental sulfur

**Ali Mohamadalizadeh*,†, Jafar Towfighi*, Alimorad Rashidi**, Mehrdad Manteghian*, Ali Mohajeri***, and Rohollah Arasteh****

*Department of Chemical Engineering, Tarbiat Modares University, P. O. Box 14115-143, Tehran, Iran
**Nanotechnology Research Center, Research Institute of Petroleum Industry, Iran
***Gas division, Research Institute of Petroleum Industry, Iran
(*Received 10 May 2010 • accepted 15 November 2010*)

**Abstract**−Modified bentonites were used for the oxidation of $H_2S$ into elemental sulfur. Active phases such as iron and cobalt sulfide were added to supports Cloisite 30B and 15A. The produced nano adsorbents were characterized by X-Ray diffraction, ICP, BET surface area and SEM. Selective oxidation of $H_2S$ was carried out over the nano adsorbent in the experimental setup. The tests were performed at 70 and 180 °C, under atmospheric pressure and in the presence of 5,000 ppm of $H_2S$ in the inlet gas stream. The results confirmed the increase in the distribution of active metals and activity of Cloisite 30B, in comparison with Cloisite 15A. Cobalt-containing support showed significant improvement in the capacity of $H_2S$ removal, and in the outlet stream less than 50 ppm of $H_2S$ was detected.

Key words: Hydrogen Sulfide, Modified Bentonite, Iron Sulfide, Cobalt Sulfide, Adsorption

## INTRODUCTION

Hydrogen sulfide is a highly poisonous and corrosive gas that causes serious damage to process equipment. There are various methods to remove hydrogen sulfide from gas streams which fall into three major categories: chemical reaction methods, absorption methods and adsorption methods. Today, the most conventional processes to remove hydrogen sulfide are amine aqueous solutions, Claus process and the liquid redox process [1-3].

Sulfur recovery unit, also named the Claus unit, is the most common method for oxidation of $H_2S$ into elemental sulfur and the high temperature Super Claus process working at temperatures above the sulfur dew point has efficiencies of about 99.5% [4-7].

Recently, some catalytic processes for selective oxidation of $H_2S$ into elemental sulfur have been developed. Selective oxidation of $H_2S$ into elemental sulfur using $TiO_2/SiO_2$ catalysts with stoichiometric amount of oxygen has been investigated and has shown good activity [8].

Metal oxides such as $Fe_2O_3$ are used in the oxidation of $H_2S$, and a high selectivity into elemental sulfur, above the sulfur dew point in the presence of a large amount of oxygen and steam, was observed [9].

Another investigation has shown that SiC-supported iron catalysts at temperature above the sulfur dew point stands high reaction temperatures without lowering selectivity. High concentration of $H_2S$ could be treated over this without deactivation of catalyst [10].

Direct oxidation at lower temperatures, in the presence of a catalyst, is another method for removal of $H_2S$. Activated carbon is widely used as the support material, because of its surface area, microporosity, high sorption capacity and easily modifiable surface properties [11-14].

Catalytic oxidation on impregnated activated carbon leads to highly efficient removal of sulfur with a high sulfur capacity of up to 60% (g/g Cat) [15].

Hydrogen-kaolinite, hydrogen-montmorillonite and hydrogen-illite clay minerals were also used to remove sulfur compounds [16]. Numerous researchers have been working on the application of adsorbing materials, on the basis of surface modified clay [17-19]. The effect of bentonite clay binders containing copper, zinc or iron in the interlayer spaces on the performance of adsorbents, in the process of hydrogen sulfide removal, has also been investigated [20].

Introduction of different metals to the structure of clays is found to result in such changes of their adsorptive properties that make it possible to use them in the removal of organic and inorganic materials [21]. Qualitative and quantitative analyses were carried out on modified Betonies [22].

Sulfides of some metals such as iron, nickel, cobalt and molybdenum can be used as catalysts for selective oxidation of $H_2S$ into elemental sulfur. In the present research, iron and cobalt sulfides have been deposited on Cloisite 15A and Cloisite 30B supports and the resulting catalyst has been employed in the process of $H_2S$ removal from gas stream.

## EXPERIMENTAL

### 1. $H_2S$ Oxidation Setup

Selective oxidation of $H_2S$ was carried out in an apparatus working isothermally under atmospheric pressure. A schematic flow diagram of the catalytic oxidation process is shown in Fig. 1. The fixed-bed reactor used for this study was constructed from a stainless steel-316 tube of 12.5 mm i.d. and 450 mm length. The gas mixture was passed downwards through the catalytic bed. The reactor was vertically mounted in an electrical furnace; the temperature was controlled by a thermal indicator controller. The flow rates of the gases ($O_2$, He, $H_2S$) were monitored and controlled with Bronkhorst mass flowmeters linked to JUMO (dTRON 304) electronic control units. The oxidation of $H_2S$ was studied at 70 and 180 °C using $H_2S$ contents of 5,000 ppm, $O_2$ (3 vol%), $H_2O$ (25 vol%) and balanced He.

†To whom correspondence should be addressed.
E-mail: alizadehsa@ripi.ir

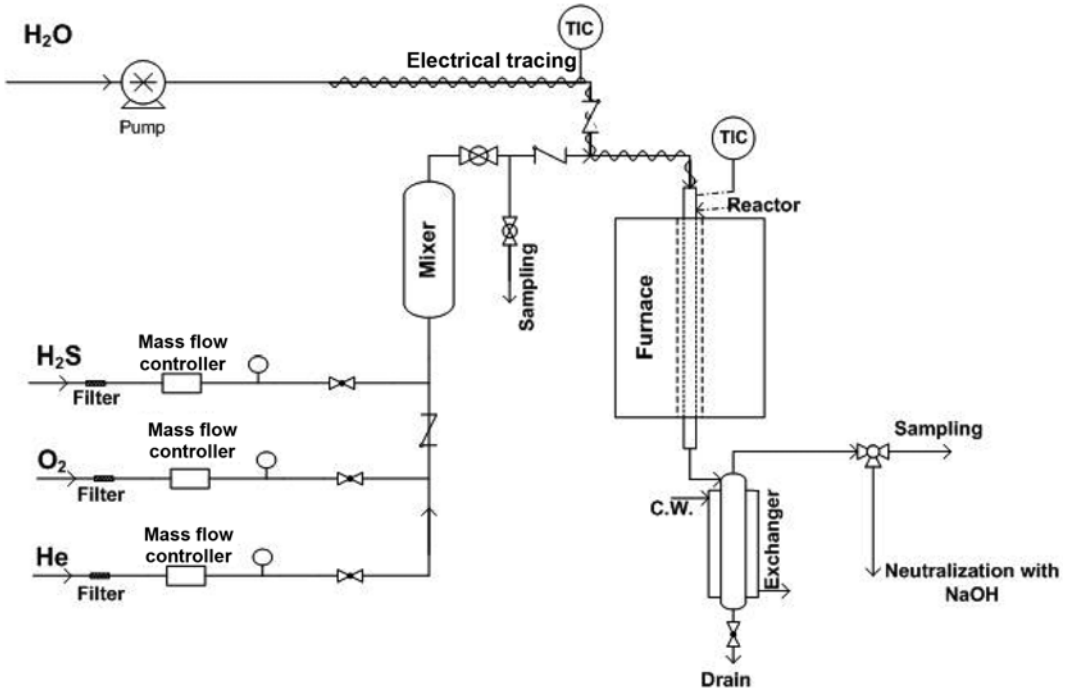


**Fig. 1. Schematic diagram of experimental system.**

A total flow of 500 ml/min was used with a GHSV of 4,000 $h^{-1}$. All lines were maintained at 120 °C with electrical tracing tapes to avoid any condensation before the analysis.

The catalyst was heated from room temperature to the reaction temperature (heating rate of 5 °C $min^{-1}$) in the presence of He. At this point the reactant flow was added.

**2. Characterization Techniques**

Scanning electron microscopy (SEM) images were obtained with a Philips, XL30 device. Gold was used as a conductive material for sample coating. The pore size and surface area measurements were performed with a Micromeritics ASAP 2010 instrument by adsorption of nitrogen at 77 K. The metal loading, analyzed by atomic absorption spectroscopy (AAS) at the analysis center of research institute of petroleum industry (Tehran, Iran) showed 10 wt% of Fe and Co. X-ray diffraction measurements were conducted using standard powder diffraction procedure carried out with a Philips diffractometer (PW-1840) (Lump 3uk$\alpha$, $\lambda$=1.54A°). TEM images were obtained with a Philips, CM 200 device. The sulfur content was determined with a high temperature measurement of sulfur content using IR detector and UOP 864 method with a LECO CS600 at the analysis center of the research institute of petroleum industry. $H_2S$ concentration was analyzed using a Mettler potentiometer (DL 70 ES), with an accuracy of ±1% of ±1 mL equipped with an Ag-$Ag_2S$ electrode (DM 141-SC) and UOP 163 method with detection threshold of 0.5 ppm.

**3. Catalyst Preparation**

Nanoclay, Cloisite 15A and 30B were supplied by Southern Clay Company, Gonzales, Texas. It is a natural montmorillonite modified with a quaternary ammonium salt (Fig. 2, where T is Tallow; C18 (65% approx.), C16 (30% approx.) and C14 (5% approx.) and HT is hydrogenated Tallow).

Iron was introduced using an incipient wetness impregnation of

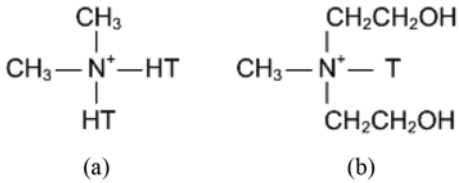


**Fig. 2. Surfactant used in manufacturing (a) Cloisite 15A, (b) Cloisite 30B.**

Cloisite 30B and 15A by a solution of iron nitrate. To achieve a homogeneous impregnation of iron nitrate on clay, iron nitrate was first dissolved in water using a heater-stirrer under mild heating, and the clay was gradually added thereto. After complete soaking of the particles in the solution, it was stirred for an extra 20 minutes. To achieve a proper dispersion of the nano particles in the solution and to increase the distance between the nano clay layers the solution was sonicated under amplitude of 90% with a pulse cycle of 1. After these steps and the complete deposition of the iron solution on the nano material, the mixture was heated and kept at 100 °C for about 1.5 hours while being stirred. After evaporation of some water content of the solution and in order to dry out the solution, the sample vessel was placed in an oven at 100 °C for 24 hours. The resulting material was calcinated in up to 450 °C, for one hour with a temperature slope of 5 °C/min and then sulfidized for 1 hour. A similar method was used to deposit cobalt sulfide nano particles on Cloisite 15A and Cloisite 30B supports.

## RESULTS

**1. Effect of Catalyst Supports**

As demonstrated in the XRD patterns of Fig. 3, iron and cobalt

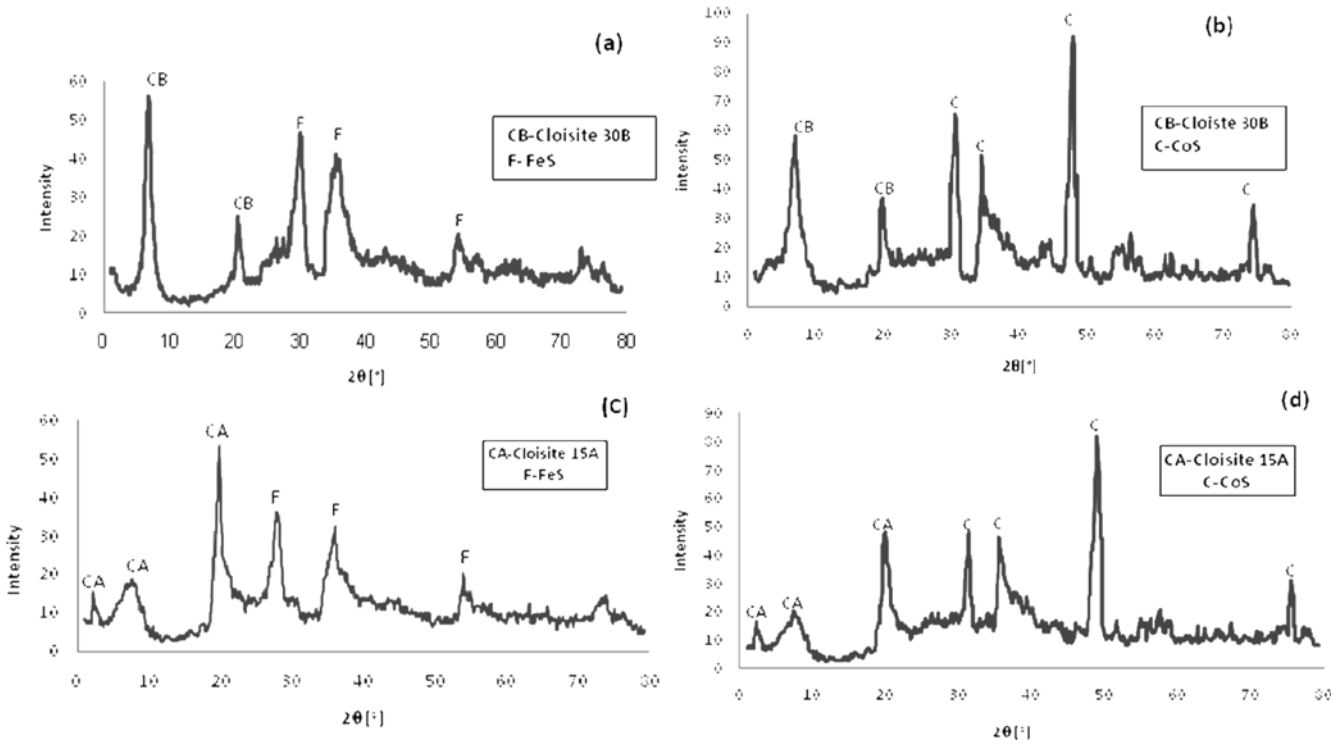


**Fig. 3. XRD patterns (a) FeS-Cloisite 30B, (b) CoS-Cloisite 30B, (c) FeS-Cloisite 15A and (d) CoS-Cloisite 15A.**

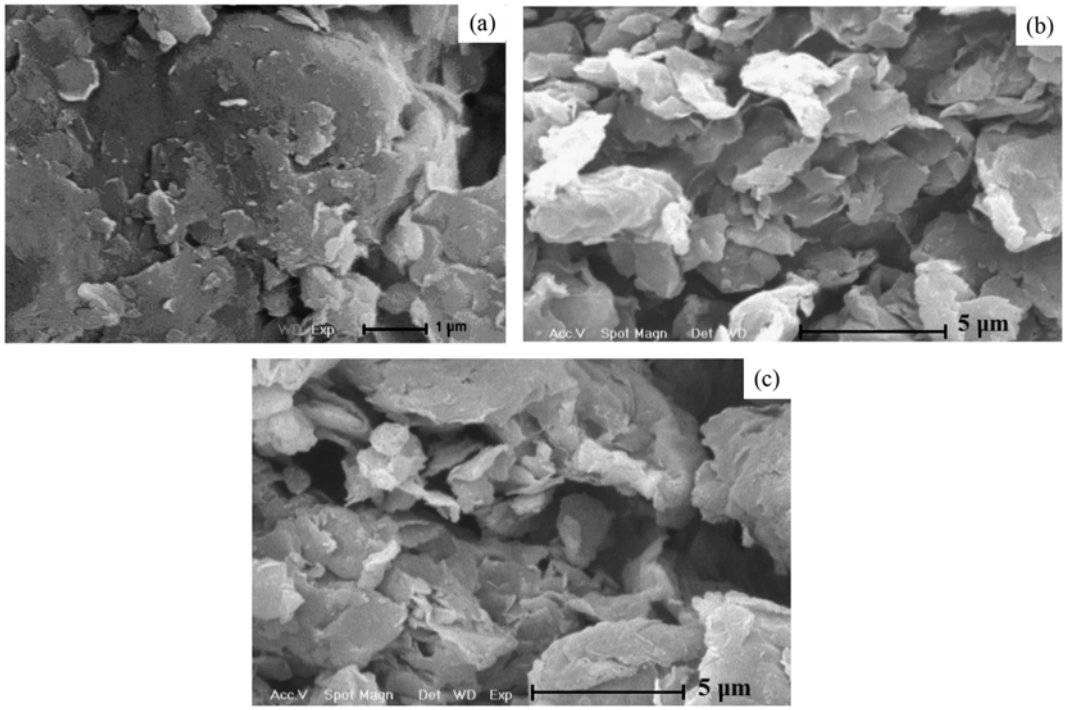


**Fig. 4. The surface of (a) Cloisite/30B, (b) Cloisite/30B-FeS before test and (c) Cloisite/30B–FeS after test with $H_2S$.**

sulfides were deposited on Cloisite 15A and Cloisite 30B supports.

The surface of Cloisite/30B-FeS is displayed before and after test with $H_2S$ in Fig. 4. For Cloisite 30B, particles were aggregated, but the amount of aggregation was decreased by modification of the surface of Cloisite 30B. Indeed, some weak links between layers were broken so the surface of Cloisite/30B-FeS (Fig. 4(b)) differed from original Cloisite 30B (Fig. 4(a)). After oxidation of $H_2S$ into elemental sulfur, the surface did not change basically (Fig. 4(c)) in comparison with the prior stage.

XRD patterns for the samples after the reaction of $H_2S$ oxida-

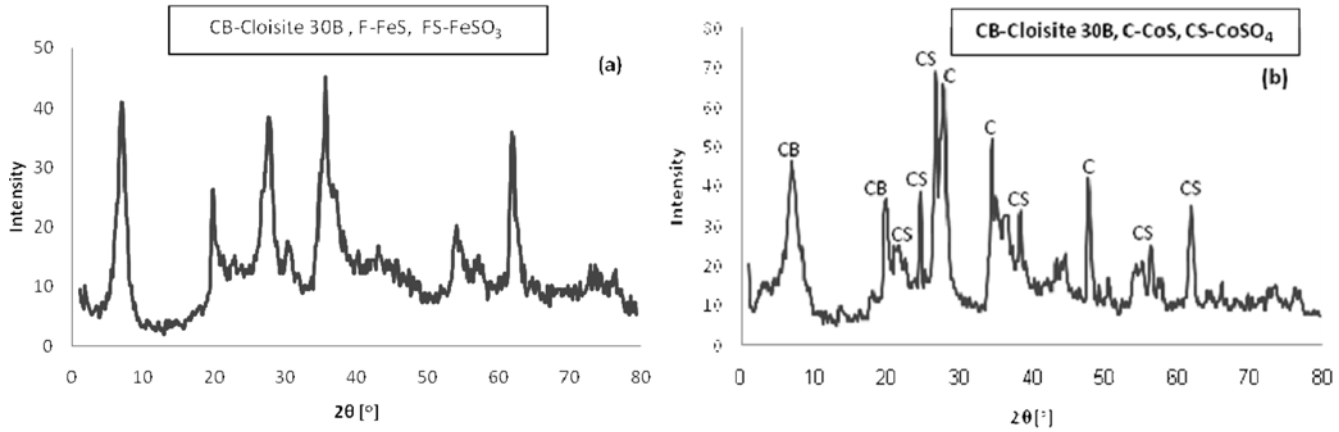


**Fig. 5. XRD patterns for samples after the reaction of $H_2S$ oxidation (a) iron compounds on Cloisite 30B and (b) cobalt compounds on Cloisite 30B.**

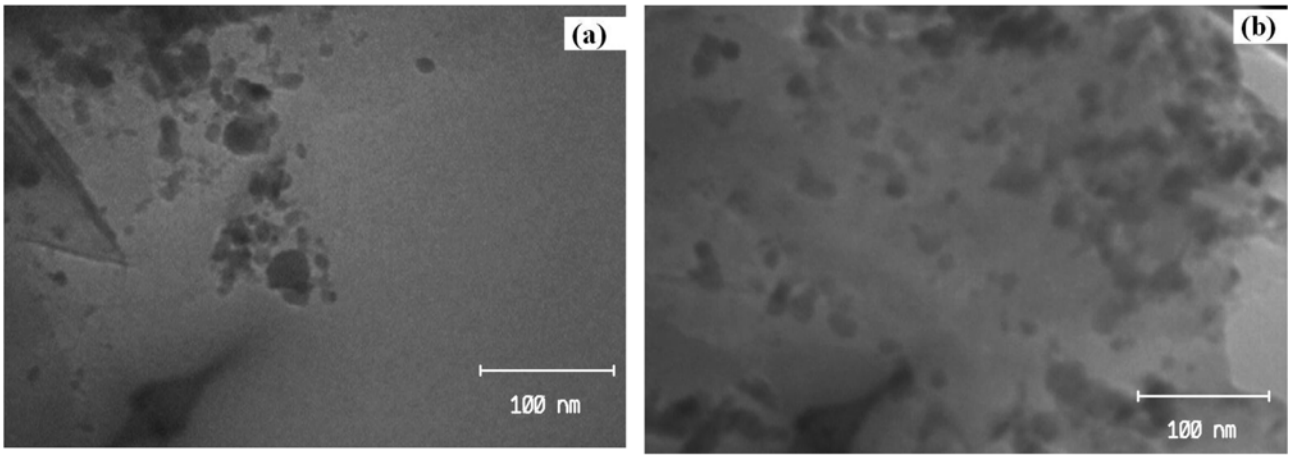


**Fig. 6. TEM images showing iron sulfide nano particles decorating the (a) Cloisite 15A and (b) Cloisite 30B.**

tion were obtained and results demonstrate iron sulfite ($FeSO_3$) and cobalt sulfate ($CoSO_4$) are created on the surface of support materials in addition to iron and cobalt sulfide (Fig. 5). It means after the reaction and in the presence of excess oxygen some metal sulfides turn into metal sulfite or sulfate.

For Cloisite 30B, water vapor washes out the sulfur particles and the catalytic sites are regenerated, while Cloisite 15A acts differently and the weight percent of sulfur in the catalyst phase is more after the reaction. Regarding the type of employed nanoclay, the inter-surface modification applied by the supplying company is believed to have an important role on the wetting quality and on homogeneous dispersion and impregnation of the metal salt. This is why hydrophobic behavior is observed for Cloisite 30B, depending on the type and nature of the functional groups applied to modify the surface properties. On the other hand due to the presence of the hydrophilic $CH_2CH_2OH$ groups in the compounds used for the modification of Cloisite 30B, the hydrophilic behavior of the material leads to a better homogeneity of the impregnation of metal salt as compared to Cloisite 15A [23].

As an example, TEM images for iron sulfide nano particles, decorated on Cloisite 15A and Cloisite 30B are shown in Fig. 6. Active sites for catalytic reaction are specified as dark points in these images. As it is clear active sites have better distribution in Cloisite 30B (Fig. 6(b)) rather than Cloisite 15A (Fig. 6(a)).

Metal catalysts have better distribution in Cloisite 30B rather than Cloisite 15A; the oxidation of $H_2S$ is enhanced on catalyst-based Cloisite 30B. The sulfur particles are washed off smoothly as the steam flow increases, so active phase lifetime is elongated. Table 1 contains data of fresh and sulfided samples and it is clear that the decrease in surface area is more severe in Cloisite 30B rather than Cloisite 15A, since condensed vapor readily washes off elemental sulfur continuously from the surface of Cloisite 30B as it was observed previously due to hydrophilic behavior of Cloisite 30B [23].

**Table 1. BET surface area of fresh and sulfide samples**

| Adsorbent | BET surface area ($m^2\ g^{-1}$) | Loss rate, % |
|---|---|---|
| Fe-15A | | |
| Fresh | 31.5 | 83 |
| Sulfided | 5.3 | |
| Fe-30B | | |
| Fresh | 25.7 | 67 |
| Sulfided | 8.5 | |

**Table 2. Total sulfur analysis**

| Sample name | Steam in feed % | Wt% sulfur |
|---|---|---|
| Clay 15A/Fe, after test | 0 | 12.41 |
| Clay 15A/Fe, after test | 20 | 11.15 |
| Clay 30B/Fe, after test | 0 | 6.64 |
| Clay 30B/Fe, after test | 20 | 3.96 |

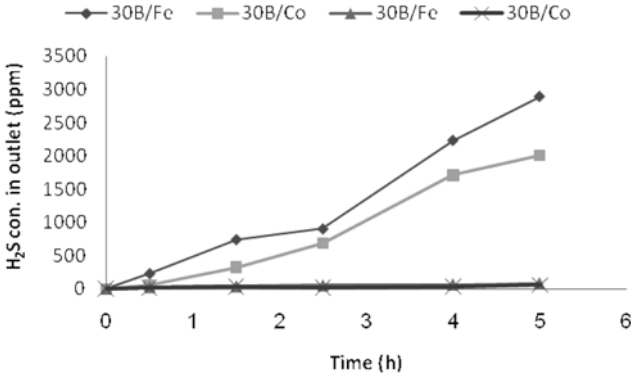


**Fig. 7. Experimental data for oxidation of $H_2S$ over catalyst at atmospheric pressure, T=180 °C (▲, ×), T=70 °C (◆, ■), GHSV=4,000 $h^{-1}$, $H_2S$ content=5,000 ppm; $O_2$ (3 vol%), balanced He and total flow=500 ml/min.**

Upon the completion of the reaction the weight percentage of remaining sulfur particles in catalytic bed is significantly lower than the no-steam case. Therefore, washing the produced sulfur leads to more free catalyst sites, facilitating the reaction (Table 2).

**2. Effect of Temperature**

The concentration of $H_2S$ in the outlet is plotted versus time at 70 °C and 180 °C for iron sulfide and cobalt sulfide catalyst supported on Cloisite 30B in Fig. 7. The oxidation of $H_2S$ is an exothermic reaction and highly thermodynamically favorable to product side (chemical equations 1 and 2):

$$H_2S = \frac{3}{2}O_2 \rightarrow SO_2 + H_2O \quad (1)$$

$$2H_2S + SO_2 \leftrightarrow \frac{3}{x}S_x^0 + 2H_2O \quad (2)$$

The first reaction is highly exothermic and second reaction, which is sometimes referred to as the Claus reaction, is also exothermic; the extent of conversion of $H_2S$ and $SO_2$ to elemental sulfur is limited by the chemical equilibrium of the second reaction. Working at a temperature above the sulfur dew point (>180 °C) increases the rate of reactions, and the efficiency of sulfur removal will increase [9]. At lower temperatures, sulfur piles up on the surface of catalyst, which leads to higher deactivation rates. When more sulfur is deposited on the support, more active sites are blocked and mass transfer flux from the bulk to the active sites is lowered. At 180 °C and in the absence of steam, cobalt and iron sulfide catalysts supported on Cloisite 30B have almost the same efficiency, but at 70 °C cobalt sulfide has a significant higher conversion of $H_2S$ to elemental sulfur.

**3. Effect of Humidity**

The effect of the presence of water vapor on oxidation was studied. The results are presented at 70 °C and 180 °C (Figs. 8 and 9). The results show that in the presence of water vapor in the feed and thus the creation of water films, the amount of $H_2S$ in outlet stream is decreased significantly. The presence of a water film enables the dissociation of $H_2S$ molecules to hydrogen sulfide ions ($HS^-$), which are then oxidized. This beneficial effect of water vapor was also observed in the literature [24,25]. In the presence of steam, catalyst

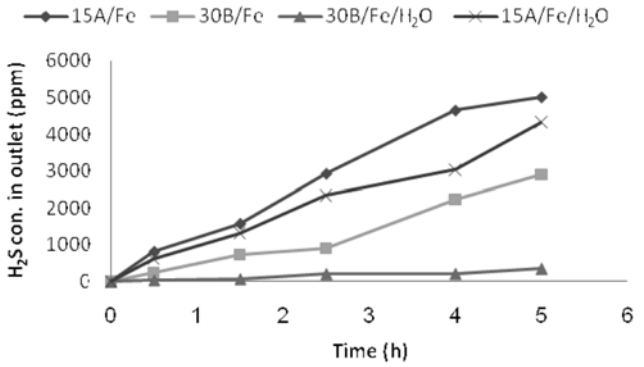


**Fig. 8. Effect of water vapor in oxidation of $H_2S$ to elemental sulfur, T=70 °C, GHSV=4,000 $h^{-1}$, total flow=500 ml/min, $H_2S$ content=5,000 ppm; $O_2$ (3 vol%), (▲, ×) $H_2O$=25 vol%, (◆, ■) $H_2O$=0 vol%, Fe loading=10 wt%.**

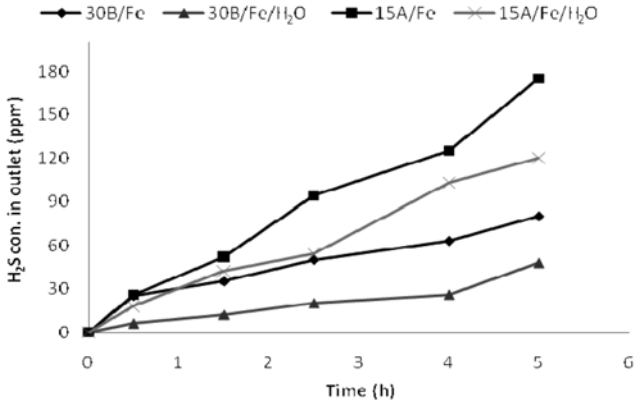


**Fig. 9. Effect of water vapor in oxidation of $H_2S$ to elemental sulfur, T=180 °C, GHSV=4,000 $h^{-1}$, total flow=500 ml/min, $H_2S$ content=5,000 ppm; $O_2$ (3 vol%), (▲, ×) $H_2O$=25 vol%, (◆, ■) $H_2O$=0 vol%, Fe loading=10 wt%.**

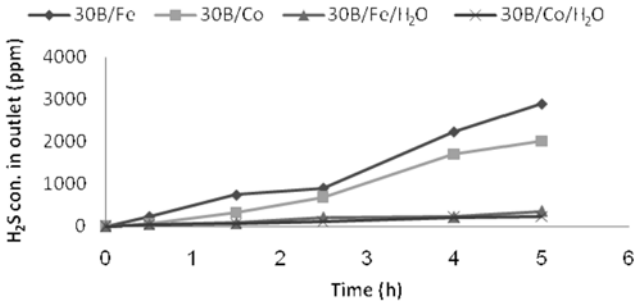


**Fig. 10. Effect of water vapor in oxidation of $H_2S$ to elemental sulfur, T=70 °C, GHSV=4,000 $h^{-1}$, total flow=500 ml/min, $H_2S$ content=5,000 ppm; $O_2$ (3 vol%), (▲, ×) $H_2O$=25 vol%, (◆, ■) $H_2O$=0 vol%, metal loading=10 wt%.**

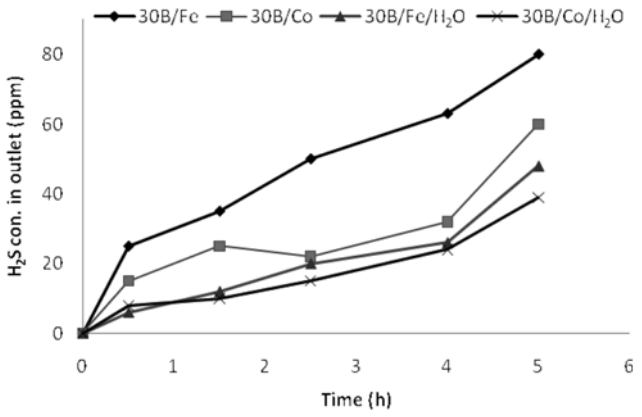


**Fig. 11. Effect of water vapor in oxidation of $H_2S$ to elemental sulfur, T=180 °C, GHSV=4,000 $h^{-1}$, total flow=500 ml/min, $H_2S$ content=5,000 ppm; $O_2$ (3 vol%), (▲, ×) $H_2O$=25 vol%, (◆, ■) $H_2O$=0 vol%, metal loading=10 wt%.**

supported on Cloisite 30B can convert more $H_2S$ to elemental sulfur rather than catalyst supported on Cloisite 15A at both 70 °C and 180 °C (Figs. 10 and 11). According to this observation, one should expect the continuous cleaning of active phase located on Cloisite 30B, which improves the performance of this catalyst, for Cloisite 15A active sites are blocked with sulfur deposits.

## CONCLUSION

Cloisite 30B and 15A supported iron and cobalt catalyst both showed a high conversion to elemental sulfur above the sulfur dew point, in the presence of oxygen in the feed. The experimental results have indicated cobalt sulfide is more favorable than iron sulfide.

Metal catalysts have better distributions over Cloisite 30B rather than Cloisite 15A. It seems the hydrophilic behavior of the material leads to a higher homogeneity of the impregnation of the metal salt as compared to Cloisite 15A support material. The oxidation of $H_2S$ on catalysts based Cloisite 30B is enhanced and the sulfur particles are washed off smoothly as the steam flow increases, so the lifetime of the active phases is elongated for Cloisite 30B. Upon the completion of the reaction the weight percentage of the remaining sulfur particles in catalytic bed is significantly lower than if there was no steam. Therefore, washing the produced sulfur leads to more free catalyst sites and thus facilitates the reaction.

## ACKNOWLEDGEMENTS

The authors gratefully acknowledge the assistance of Dr. Miranbeyghi and Ms. Solmaz Rasoulipour from the analytical chemistry lab of Research Institute of Petrochemical Industry, for their kind assistance in carrying out measurements.

## REFERENCES

1. R. Wang, *Sep. Purif. Technol.*, **31**, 111 (2003).
2. E. Sasaoka, *Energy Fuels*, **8**, 1100 (1994).
3. M. p. Elsner, M. Menge, C. Muller and D. W. Agar, *Catal. Today*, **79**, 487 (2003).
4. P. Van Den Brink and J. W. Geus, US Patent, 5,286,697 (1994).
5. P. H. Berben and J. W. Geus, US Patent, 4,818,740 (1989).
6. L. Connock, *Sulphur*, **257**, 34 (1998).
7. L. V. A. Truong and N. Abatzoglou, *Biomass and Bioenergy*, **29**, 142 (2005).
8. S. W. Chun, J. Y. Jang, D. W. Park, H. C. Woo and J. S. Chung, *Appl. Catal. B: Environ.*, **16**, 235 (1998).
9. N. Keller, C. P. Huu and M. J. Ledoux, *Appl. Catal. A: Gen.*, **217**, 205 (2001).
10. P. Nguyen, D. Edouard, J. M. Nhut, M. J. Ledoux, C. Pham and C. P. Huu, *Appl. Catal. B: Environ.*, **76**, 300 (2007).
11. O. Conchi and T. J. Bandosz, *Energy Fuels*, **20**, 1076 (2006).
12. T. J. Bandosz and Q. Le, *Carbon*, **36**, 39 (1998).
13. A. Bagreev and T. J. Bandoz, *Carbon*, **39**, 2303 (2001).
14. L. Wang, B. Cao, S. Wang, Q. Yuan, *Chem. Eng. J.*, **118**, 133 (2006).
15. L. Wang, B. Cao, S. Wang and Q. Yuan, *Chem. Eng. J.*, **118**, 133 (2006).
16. P. G. Nahin and J. E. Sherbarne, US Patent, 2,243,049 (1960).
17. B. Krishna and D. Prakash, *Appl. Clay Sci.*, **20**, 65 (2001).
18. S. Mikhail, T. Zaki and L. Khalil, *Appl. Catal.: Gen.*, **227**, 265 (2002).
19. A. Adib, A. Bagreev and T. J. Bandosz, *Environ. Sci. Technol.*, **34**, 686 (2000).
20. D. Nguyen-Thanh and T. J. Bandosz, *Carbon*, **43**, 359 (2005).
21. D. Nguyen and T. Bandosz, *Micropor. Mesopor.*, **92**, 47 (2006).
22. K. Stepova, D. Maquarrie and I. Krip, *Appl. Clay Sci.*, **42**, 625 (2009).
23. O. Yilmaza, C. N. Cheaburub, D. Durraccioc, G. Gulumsera and C. Vasileb, *Appl. Clay Sci.*, **49**, 288 (2010).
24. A. Primavera, A. Trovarelli and P. Andreussi, *Appl. Catal.*, **173**, 185 (1998).
25. J. M. Nhut, p. Nguyen, C. P. Huu, N. Keller and M. J. Ledoux, *Catal. Today*, **92**, 91 (2004).